

Magnetic turbulence suppression by a helical mode in a cylindrical geometry

J.-H. Kim and P. W. Terry

Citation: *Phys. Plasmas* **19**, 122304 (2012); doi: 10.1063/1.4769369

View online: <http://dx.doi.org/10.1063/1.4769369>

View Table of Contents: <http://pop.aip.org/resource/1/PHPAEN/v19/i12>

Published by the [American Institute of Physics](#).

Related Articles

Effect of secondary convective cells on turbulence intensity profiles, flow generation, and transport
Phys. Plasmas **19**, 112506 (2012)

Asymmetric chiral alignment in magnetized plasma turbulence
Phys. Plasmas **19**, 112301 (2012)

Three-dimensional modeling of beam emission spectroscopy measurements in fusion plasmas
Rev. Sci. Instrum. **83**, 113501 (2012)

An electromagnetic theory of turbulence driven poloidal rotation
Phys. Plasmas **19**, 102311 (2012)

Short wavelength ion temperature gradient turbulence
Phys. Plasmas **19**, 102508 (2012)

Additional information on Phys. Plasmas

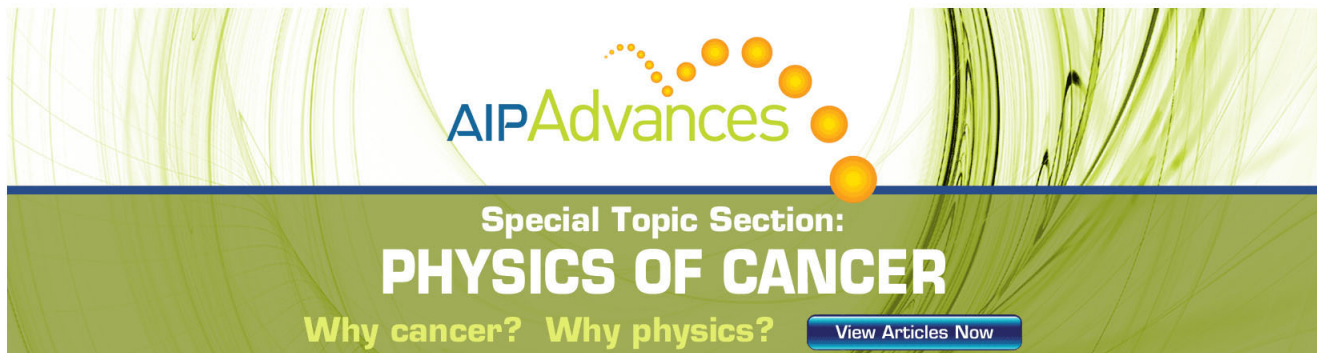
Journal Homepage: <http://pop.aip.org/>

Journal Information: http://pop.aip.org/about/about_the_journal

Top downloads: http://pop.aip.org/features/most_downloaded

Information for Authors: <http://pop.aip.org/authors>

ADVERTISEMENT



AIP Advances

Special Topic Section:
PHYSICS OF CANCER

Why cancer? Why physics? [View Articles Now](#)

Magnetic turbulence suppression by a helical mode in a cylindrical geometry

J.-H. Kim^{a)} and P. W. Terry

Department of Physics and Center for Momentum Transport and Flow Organization, University of Wisconsin-Madison, Madison, Wisconsin 53706, USA

(Received 12 September 2012; accepted 13 November 2012; published online 7 December 2012)

To study processes involved in a helical structure formation in reversed field pinch devices, the scaling of a turbulent boundary layer width associated with a vortex structure having large shears of magnetic field and flow is obtained for reduced magnetohydrodynamics. The coherent vortex, with its flow and magnetic shears, interacts with Alfvén turbulence, forming a turbulent boundary layer at the edge of the vortex. The layer arises from the balance between turbulence diffusion rates and shearing rates and suppresses the turbulence in the structure. The suppression of turbulence impedes relaxation of the coherent vortex profiles, leading to long coherence times. The scaling of the boundary layer width reveals that both magnetic shear and flow shear can effectively suppress magnetic turbulence. © 2012 American Institute of Physics. [<http://dx.doi.org/10.1063/1.4769369>]

I. INTRODUCTION

Recently an operating mode of the reversed field pinch (RFP) known as the quasi single helicity state (QSH)^{1–3} has attracted attention for its favorable confinement properties.^{2,4} It is characterized by a toroidal mode spectrum in which one mode (typically corresponding to the innermost resonant tearing mode of toroidal mode number $n = n_0$) has much more energy than modes with $n > n_0$. In contrast, under ordinary multiple helicity operation the n_0 mode and other modes have comparable energy. When the spectrum is dominated by a single mode, this mode becomes highly coherent, or quasi-stationary, and imparts a helical character to the equilibrium. The coherence indicates that nonlinear interactions with other modes, which normally produce decorrelation in a nonlinear timescale, are suppressed. Moreover, there is evidence for a thermal transport barrier at the edge of the helical core formed by the dominant helicity.^{2,4} The QSH state is favored by large current. In RFX-mod⁵ the system oscillates between QSH and multiple helicity states, spending more time in QSH relative to the multiple helicity configuration if the current is high.³

A Hamiltonian theory⁶ of the magnetic field has shown that a large single helicity fluctuation relative to other helicities results in a unitary helical equilibrium core without an x -point, as observed in experiment. However the dominance of a single helicity is imposed *ad hoc* in the theory, and there is no treatment of the interactions that take place among tearing modes. While numerical modeling^{7,8} of multiple tearing modes has produced a situation in which the innermost helicity becomes dominant, this only occurs at low Hartman number, through collisional stabilization of outer modes relative to the less collisional innermost mode. However, the high current conditions of QSH imply high Hartman number, not the opposite, and would only provide stabilization at the extreme edge. It is worthwhile exploring other mechanisms for sustaining QSH that are valid for high magnetic Reynolds

number (or high current), that address transport-barrier-like properties, and that have connections to limit cycle behavior.

This paper considers how shear associated with the dominant helicity fluctuation affects the other fluctuations with which it interacts, and what conditions might allow it to become coherent by suppressing the other helicities. The complexities of the phenomenon preclude a theory that treats the RFP spectrum in realistic detail; consequently, we explore basic workings. Tearing modes have flow,⁹ and that flow is radially sheared. It is well known that equilibrium shear flows suppress turbulence and transport driven by other equilibrium gradients.^{10–13} Moreover, it has also been shown that the shear flow of one vortical fluctuation in 2D Navier-Stokes turbulence can suppress surrounding turbulence, provided its vorticity exceeds a threshold relative to the vorticity of ambient fluctuations.^{14–16} The result is that the vortical fluctuation becomes coherent, suffering virtually no decay from interactions with the turbulence. This type of behavior is consistent with the coherence of the dominant helicity in the QSH state. However, tearing modes and the RFP global fluctuation spectrum are more magnetic than electrostatic. Consequently, analysis of the effect of shear on turbulent interactions needs to include magnetic shear.¹⁷

The magnetic shear of a dominant filamentary current fluctuation can in fact suppress interacting fluctuations and has been shown to lead to the type of intermittency inferred in interstellar turbulence from pulsar scintillation.¹⁸ The effect was shown for kinetic Alfvén wave (KAW) turbulence, a type of electron-compressible magnetic turbulence in which flow plays no dynamical role. Tearing modes, in contrast, are modeled at the minimum with MHD, and flow is essential to their dynamics. Therefore, in considering the tearing mode fluctuations relevant to QSH, shear of both the flow and the magnetic field must be treated in a system like MHD.

Magnetic shear, when treated as a property of linear stability, is known to abet suppression by flow shear in internal transport barriers.^{12,19} When the combination of magnetic shear and flow shear influence nonlinear dynamics, the effect is more complex. At a minimum, two inhomogeneities that

^{a)}Electronic mail: jkim282@wisc.edu.

are not linked in some simple ways complicate the mode structure of fluctuations.²⁰ In a quasilinear turbulence closure of MHD the nonlinear effect of magnetic shear is found to oppose the suppressing effect of strong flow shear.²¹ On the other hand, magnetic shear can suppress tokamak turbulence nonlinearly.²² In light of these complexities we will emphasize the interaction between flow shear and magnetic shear and will employ an approach that is sufficiently general to offer insight on the situation.

To produce as clear a view as possible of the nonlinear effect of the magnetic shear and flow shear of a dominant fluctuation on ambient MHD turbulence, we replace the unstable tearing modes of the low- q RFP magnetic equilibrium with idealized magnetic fluctuations. The fluctuation of the dominant helicity in the QSH state is represented by a fluctuation labeled the current vortex. It has both a flow and magnetic field whose radial variation is like that of an RFP tearing mode. At the level of the interaction of turbulence and shear, the helicity of the dominant mode is not an essential feature (that is not to say it would not have some effect). Hence we treat the dominant mode as having azimuthal and axial symmetry, i.e., with mode numbers $n = m = 0$. The calculation is not embedded in the specifics of the RFP q profile; hence, the current vortex should not be thought of as a structure at the reversal surface. The other helicities of the QSH state are represented as Alfvénic fluctuations with $n, m > 0$. For tractability, all fluctuations are treated under the reduced MHD approximation. This is obviously an idealization of the physics in the QSH state. Hence this work should not be considered a model of QSH, but a basic study of how magnetic and flow shears jointly operate for interactions that can be expected in QSH.

There is also a geometrical difference between rotating helical and vortex structures. While the rotating vortex ($m = n = 0$) presents a constant shear to the turbulence, the helical structure presents oscillating shear to the turbulence, such that the net effect should be averaged. However, this oscillating shear effect will not be significant at the large shear limit where the linear shearing occurs at a fraction of the rotation period.

The ambient fluctuations live in the strongly inhomogeneous environments of the current vortex. Both their magnitudes and radial structures are dictated by the shears of the current vortex. When the shears are large, the radial variation of ambient structures is confined to a boundary layer. Asymptotic analysis provides a formal ordered set of approximations that enable analysis. This boundary layer analysis has been employed in both the Navier-stokes¹⁵ and kinetic Alfvén wave turbulence¹⁸ problems mentioned earlier and is used here in an analogous way. Some background on the boundary layer analysis will be presented in Sec. II.

The main conclusion of this paper is that in the limit of large magnetic shear and flow shear, the turbulent boundary layer width Δr is inversely proportional to the 1/3 power of an effective shear, $(\Omega'_{\text{eff}})^{-1/3}$. The effective shear combines the shears of the flow and magnetic field. Two limits conceptually characterize the combination. In one, the shears combine linearly, so that one shear can either enhance the suppression of the other or weaken it, depending on their rel-

ative directions and the turbulence characteristics. In the other limit the shears combine quadratically, and one always weakens the effect of the other, regardless of relative direction. When there is significant suppression, the current vortex becomes coherent. The scaling of its lifetime normalized to a tearing interaction time in the presence of shearing effects strongly depends on the plasma current, making coherence stronger for larger current. This is consistent with QSH observations and provides a possible explanation for the favorability of QSH with high current operation.

This paper is organized as follows: a theoretical formulation, the large shear approximation, the concept of boundary layer formation, and eddy-damped quasi-normal Markovian (EDQNM) closure are presented in Sec. II. The dimensional analysis of turbulent boundary layer is given in Sec. III. The time scale of coherent structures is estimated in Sec. IV. Section V gives the conclusion and the discussion.

II. THEORETIC FRAMEWORK

A. Reduced MHD

To describe the interaction of fluctuations in MHD turbulence in a plasma with a strong mean field, a reduced description is highly advantageous. Reduced MHD²³ provides the advantage of simplicity of description while allowing the effect of shear in fluctuating flows and magnetic fields to be investigated in detail. The dimensionless equations apply under the assumption of $\mathbf{B}_0(\mathbf{x}) = B_z \hat{z}$ and are given by

$$\frac{d\omega}{dt} + \nabla_{\parallel} j = 0, \quad (1a)$$

$$\frac{\partial \psi}{\partial t} + \nabla_{\parallel} \phi = 0. \quad (1b)$$

Here $\omega = \nabla_{\perp}^2 \phi$ is the vorticity, $j = \nabla_{\perp}^2 \psi$ is the current (defined in the opposite direction of the true current), and the parallel and total derivatives are

$$\nabla_{\parallel} f = \hat{\mathbf{b}}_0 \cdot \nabla f - [\psi, f] = \frac{\partial f}{\partial z} - [\psi, f],$$

$$\frac{df}{dt} = \frac{\partial f}{\partial t} + [\phi, f],$$

and

$$[f, g] = \frac{1}{r} \left(\frac{\partial f}{\partial r} \frac{\partial g}{\partial \theta} - \frac{\partial f}{\partial \theta} \frac{\partial g}{\partial r} \right).$$

The magnetic potential ψ and the electrostatic potential ϕ are symmetric: Eq. (1a) has the nonlinear terms, $[\psi, j]$ and $[\phi, \omega]$, and Eq. (1b) has $[\psi, \phi]$. In a cylindrical geometry, an ansatz with the periodicity in the azimuthal and axial directions gives

$$f(r, \theta, z, t) = \sum_{m,k} f_{mk}(r, t) e^{i(m\theta - kz)}.$$

Equations (1a) and (1b) have a linear solution describing two Alfvén waves moving in the opposite axial directions.

We will split the fluctuations into a slowly evolving component f_0 with mode numbers m_0 and k_0 and a rapidly evolving component with $m > m_0$ and $k > k_0$,

$$f = f_0 + \tilde{f}. \quad (2)$$

It is assumed that the slow mode (m_0, k_0) is dominant, i.e., $f_0 \gg \tilde{f}$. Hence the slow mode represents the dominant helicity of the QSH state, while the fast modes represent other helical modes. We derive conditions under which the fluctuation with (m_0, k_0) suppresses nonlinear interactions with other fluctuations, making it long-lived and justifying *a posteriori* the assumption that it is slowly evolving. The fast time scale is the time scale of the nonlinear interaction of tearing modes (turbulent correlation time) in a multiple helicity situation. Because the nonlinear interaction saturates the instability, the time scale is the hybrid tearing instability time scale. The slow time scale is much longer, representing mixing of the dominant mode structure by fluctuations that

have been suppressed by the shear of the magnetic-field and flow of the dominant mode.

For the dominant slowly evolving mode $(m_0, k_0) = (0, 0)$, the evolution of $\tilde{f} = f_{m_0 k_0} = f_{00}$ is described by equations for the vorticity and flux of the mode

$$\frac{\partial \tilde{\omega}}{\partial t} = - \sum_{k', m'} \left[\frac{im'}{r} \left(\frac{\partial \tilde{\phi}'^*}{\partial r} \tilde{\omega}' - \frac{\partial \tilde{\omega}'^*}{\partial r} \tilde{\phi}' \right) - \frac{im'}{r} \left(\frac{\partial \tilde{\psi}'^*}{\partial r} \tilde{j}' - \frac{\partial \tilde{j}'^*}{\partial r} \tilde{\psi}' \right) \right], \quad (3a)$$

$$\frac{\partial \tilde{\psi}}{\partial t} = \sum_{k', m'} \frac{im'}{r} \left(\frac{\partial \tilde{\psi}'^*}{\partial r} \tilde{\phi}' - \frac{\partial \tilde{\phi}'^*}{\partial r} \tilde{\psi}' \right), \quad (3b)$$

where $\tilde{f}'^* = \tilde{f}'_{-m', -k'}$ and $\tilde{f}' = \tilde{f}'_{m' k'}$ are rapidly evolving, subdominant turbulent helical modes. The evolution equations for the subdominant turbulent fluctuations $\tilde{f} = \tilde{f}'_{mk}$ are

$$\frac{\partial \tilde{\omega}}{\partial t} + ik\tilde{j} + \frac{im}{r} \left[\left(\frac{d\tilde{\phi}}{dr} \tilde{\omega} - \frac{d\tilde{\omega}}{dr} \tilde{\phi} \right) - \left(\frac{d\tilde{\psi}}{dr} \tilde{j} - \frac{d\tilde{j}}{dr} \tilde{\psi} \right) \right] - \sum_{\substack{m' + m'' = m \\ k' + k'' = k}}^* \left[\frac{im'}{r} \left(\frac{\partial \tilde{\phi}''}{\partial r} \tilde{\omega}' - \frac{\partial \tilde{\omega}''}{\partial r} \tilde{\phi}' \right) - \frac{im'}{r} \left(\frac{\partial \tilde{\psi}''}{\partial r} \tilde{j}' - \frac{\partial \tilde{j}''}{\partial r} \tilde{\psi}' \right) \right], \quad (4a)$$

$$\begin{aligned} & \frac{\partial \tilde{\psi}}{\partial t} + ik\tilde{\phi} - \frac{im}{r} \left(\frac{d\tilde{\psi}}{dr} \tilde{\phi} - \frac{d\tilde{\phi}}{dr} \tilde{\psi} \right) \\ & = \sum_{\substack{m' + m'' = m \\ k' + k'' = k}}^* \frac{im'}{r} \left(\frac{\partial \tilde{\psi}''}{\partial r} \tilde{\phi}' - \frac{\partial \tilde{\phi}''}{\partial r} \tilde{\psi}' \right). \end{aligned} \quad (4b)$$

The notation is simplified by dropping (m, k) and instead using $\tilde{f}' = \tilde{f}'_{m' k'}$ and $\tilde{f}'' = \tilde{f}''_{m'' k''}$. The sum \sum^* in the nonlinear terms is done excluding the cases of $(m', k') = (m, k)$ or $(m'', k'') = (m, k)$.

The fast time scale equation has a set of terms on the LHS describing the interaction of the subdominant helical modes \tilde{f} with the dominant helicity \tilde{f} , and a set of terms of the RHS describing nonlinear interactions among the subdominant helical modes. With the time scale separation the interaction involving the dominant helicity is effectively linearized but, importantly, enters as an inhomogeneous background. When the inhomogeneity is strong the subdominant fluctuations respond by developing structure that is set by the balance of the inhomogeneous interaction terms on the LHS and the nonlinear interactions on the RHS. This structure is well known to represent a suppression of the fluctuation activity in regions where the inhomogeneity is strong.^{13,18} The slow time scale equation describes the evolution of the dominant helicity under the anomalous diffusion caused by the subdominant fluctuations. When these two sets of equations are solved, we can determine from the fast time scale equation how strong the inhomogeneity of the dominant fluctuation must be to suppress the subdominant fluctuations. The slow time scale equation provides a

measure of the time scale on which the dominant helicity is stationary. In light of this discussion, while Eqs. (4a) and (4b) contain linear Alfvén terms, the more important effect is Alfvénic propagation on the inhomogeneous background created by the dominant helicity mode.

B. Large shear approximation

We now consider the inhomogeneous interaction terms involving the dominant helicity that appear on the LHS of Eqs. (4a) and (4b). The factor $d\tilde{\phi}/dr$ represents the flow of the dominant helicity mode. The mode that is symmetric in the axial and azimuthal directions, $(m, n) = (0, 0)$, has a vortical flow with the same symmetry. The flow $d\tilde{\phi}/dr$ advects the fluctuating vorticity $\tilde{\omega}$ in the azimuthal direction. If radially sheared, this flow shears the structures associated with $\tilde{\omega}$. Nonlinearity, present because of the nonlinear terms from the RHS, introduces decorrelation of $\tilde{\omega}$. As a result, the sheared fluctuation $\tilde{\omega}$ decorrelates in the radial direction across a reduced scale ℓ'_c relative to shear-free scale ℓ_c .¹⁵ The shearing produced by the dominant vortex flow is quantified by the differential of the angular velocity. An expansion of \bar{V}_θ/r for local analysis yields the shearing rate in the first order term

$$\begin{aligned} \Omega_\phi(r) & \equiv \frac{\bar{V}_\theta}{r} = \frac{1}{r} \frac{d\tilde{\phi}}{dr} \\ & \simeq \Omega_\phi(r_0) + (r - r_0) \left(\frac{d\Omega_\phi}{dr} \right)_{r=r_0}. \end{aligned} \quad (5)$$

The expansion is valid when the shearing effect is strong in comparison to shear instability dependent on Ω_ϕ'' . Moreover,

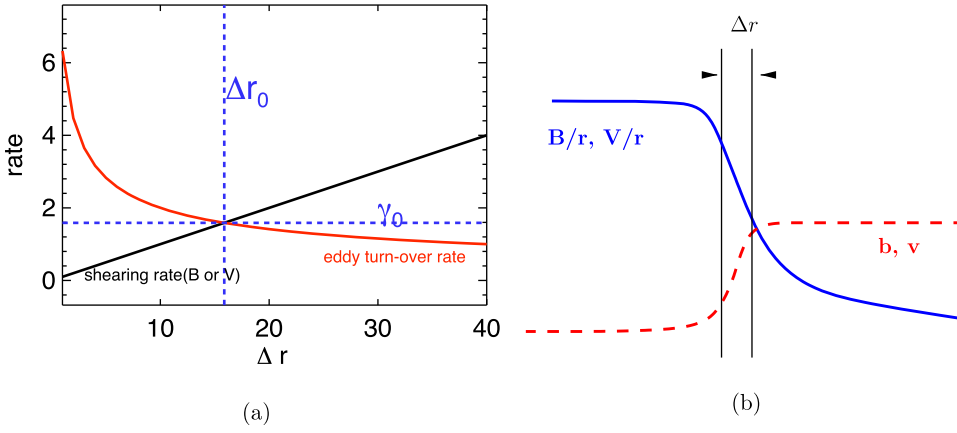


FIG. 1. Illustration of (a) the balance between shearing rate and eddy turn-over rate and (b) the resulting boundary layer formation.

the radial correlation length $\ell_v \sim \Delta r$ should be shorter than the flow scale length $\ell_\Omega \equiv (2\Omega'_\phi/\Omega''_\phi)$, where $\Omega'_\phi = d\Omega/dr$ and $\Omega''_\phi = d^2\Omega/dr^2$

Next, consider the factor $d\bar{\psi}/dr$ in Eqs. (4a) and (4b). This represents the magnetic field of the dominant helicity mode. Like the vortical flow $d\bar{\phi}/dr$ it too has radial shear. Its effect is analogous to a flow shear because the subdominant fluctuations of other helical modes have an Alfvénic character in MHD. Alfvén waves propagate along the magnetic field with velocity proportional to B . If the field is inhomogeneous in a direction along phase fronts, the differential propagation speed distorts the phase fronts as shown in Fig. 2. When the differential stretching of a phase front reaches the correlation length associated with the nonlinear interaction between helical modes, the front breaks and the radial correlation is reduced. While phase fronts are “sheared,” the process is not advective shear straining, but rather one of wave refraction. The refractive shearing produced by the magnetic field of the dominant helicity mode is quantified by the differential of an Alfvén angular velocity. An expansion of \bar{B}_θ/r for local analysis yields the refractive shearing rate in the first order term

$$\begin{aligned} \Omega_\psi(r) &\equiv \frac{\bar{B}_\theta}{r} = \frac{1}{r} \frac{d\bar{\psi}}{dr} \\ &\simeq \Omega_\psi(r_0) + (r - r_0) \left(\frac{d\Omega_\psi}{dr} \right)_{r=r_0}, \end{aligned} \quad (6)$$

for $\ell_B \sim \Delta r \ll \ell_J \equiv (2\Omega'_\psi/\Omega''_\psi)$. The background axial field B_0 is constant. The magnetic field line that a fluctuation experiences is the combination of the axial magnetic field and the azimuthal magnetic field $d\bar{\psi}/dr$. The phase front is refracted on the plane perpendicular to the axial magnetic field. The necessary condition for the local approximation, $\Delta r \ll \ell_J$ or ℓ_Ω , gives a clear limit for the approximation. When this condition is met together with $\Delta r \ll \ell_\Omega$, the key dynamical effect of the slow-time fluctuations on the other helical modes includes only linear shearing and excludes current (or flow) driven instability proportional to the second derivative of $\bar{\phi}$ or $\bar{\psi}$.

In the strong shear limit, the interaction between a mean flow shear and turbulence has long been characterized as a reduction in radial correlation length determined from the balance of shearing rate and eddy turnover rate. The two terms balance if the system remains turbulent as shear becomes large. From Fig. 1(a), in which the two rates are

plotted as functions of Δr , it is clear that Δr decreases as the slope of the shearing term (shearing rate) increases. When the shear flow is the flow of coherent structure in turbulence, Δr is the width of a boundary layer at the interface between the turbulence and the structure, inside of which the turbulence becomes evanescent and drops to very low levels, as shown in Fig. 1(b). The fluctuations inside the structure can be expressed by $v/v_{ext} \sim \Delta r/\Delta r_{ext}$ from dimensional analysis. The same concept can be applied to the boundary formation by magnetic shear, too.

The shearing rate $d\Omega_\phi/dr$ is a familiar quantity for parametrizing the strength of suppression by flow shear. The parameter enters both linear stability calculations, where flow shear can stabilize certain pressure, density, and current gradient driven instabilities, and calculations of turbulence where flow shear reduces correlation lengths and lowers fluctuation levels.¹³ Magnetic shear has long been known to stabilize certain instabilities, with $d\Omega_\psi/dr$ an appropriate measure of the magnetic shear strength. Here we observe that $d\Omega_\psi/dr$ also parametrizes a nonlinear, turbulent effect with analogous reductions of correlation length and turbulence level to those produced by flow shear. This nonlinear effect was previously studied for fluctuations of kinetic Alfvén wave turbulence.¹⁸ Here it is extended to MHD turbulence, where the nonlinear effects of $d\Omega_\phi/dr$ and $d\Omega_\psi/dr$ are considered jointly.

C. Turbulence closure equations

Now, a simple dimensional analysis is applied in order to obtain a radial decorrelation length represented in Fig. 1. Multiple balances between a shear on the LHS and nonlinear decorrelation on the RHS can be possible because there are magnetic and flow shears as well as multiple nonlinear terms in Eqs. (4a) and (4b). One balance is when the flow shear is dominant ($\Omega'_\phi \gg \Omega'_\psi$). The balance is achieved with a narrow radial correlation length Δr_a arising from the vorticity equation (4a) or Δr_b from the induction equation (4b). The application of dimensional analysis yields

$$\Delta r_a \sim \left(\frac{\tilde{\phi}}{r\Omega'_\phi} \text{Max} \left(1, \frac{\tilde{\psi}^2}{\tilde{\phi}^2} \right) \right)^{1/2} \quad \text{and} \quad \Delta r_b \sim \left(\frac{\tilde{\phi}}{r\Omega'_\phi} \right)^{1/2},$$

where $\text{Max}(1, \tilde{\psi}^2/\tilde{\phi}^2)$ represents which nonlinear term is responsible for the balance: $\mathbf{E} \times \mathbf{B}$ nonlinearity $[\tilde{\phi}, \tilde{\omega}]$ in flow

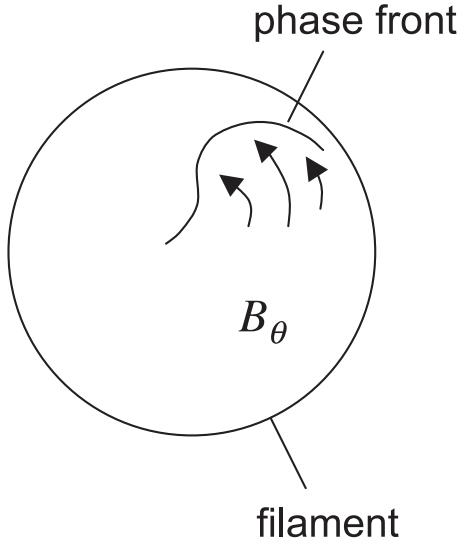


FIG. 2. Schematic description of Alfvénic fluctuation distortion by linear magnetic shear. Reprinted with permission from *Astrophys. J.* **665**, 402 (2007). Copyright 2007 IOP Publishing Ltd.¹⁸

dominant turbulence or nonlinear magnetic flutter $[\tilde{\psi}, \tilde{j}]$ in magnetic field dominant turbulence in Eq. (4a). When flow-dominant turbulence ($\tilde{\phi} \gg \tilde{\psi}$) interacts with the flow shear of the dominant helicity mode, the correlation length Δr_a becomes equivalent to the length Δr_b so that the reduced length by flow shear $\Delta r \sim \Delta r_a \sim \Delta r_b$ can be determined. Here Δr is the same as the scaling obtained in Navier-Stokes equation.¹⁵ For magnetic field dominant turbulence ($\tilde{\psi} \gg \tilde{\phi}$), the correlation length cannot be easily determined since $\Delta r_a/\Delta r_b \sim \tilde{\psi}/\tilde{\phi}$.

When the magnetic shear is dominant ($\Omega'_\psi \gg \Omega'_\phi$), a similar scaling is obtained

$$\Delta r_a \sim \left(\frac{\tilde{\psi}}{r\Omega'_\psi} \text{Max} \left(1, \frac{\tilde{\phi}^2}{\tilde{\psi}^2} \right) \right)^{1/2} \quad \text{and} \quad \Delta r_b \sim \left(\frac{\tilde{\psi}}{r\Omega'_\psi} \right)^{1/2}.$$

In the magnetic field dominant turbulence, the reduced correlation length $\Delta r \sim \Delta r_a \sim \Delta r_b$ can be estimated. This scaling $\Delta r \sim (\tilde{\psi}/r\Omega'_\psi)^{1/2}$ in the magnetic field fluctuation outside of the current vortex is not the same as the scaling obtained in kinetic Alfvén wave¹⁸ as in the Navier-Stokes equation. The difference can be attributed to the wave property that KAW is dispersive, $\omega \sim k_\perp k_\parallel$, in the radial direction while Alfvén wave is not $\omega \sim k_\parallel$. So wave characteristics are the one of the determining factors.

The dimensional analysis in the previous paragraphs could not give any insight into the scaling of the boundary width when magnetic shear is at the same order as flow shear as well as when flow fluctuations are at the equivalent amplitudes with magnetic field fluctuations even under one dominant shear, either Ω'_ψ or Ω'_ϕ . Therefore, a more systematic treatment is necessary to sort out how the balance between shear and turbulence is achieved.

One approach is to apply a statistical closure to Eqs. (4a) and (4b), consider the nonlinear interactions as nonlinear diffusion, and compare shearing rates with nonlinear diffusion rates. We consider a variant of the EDQNM closure, which

closes a statistical moment hierarchy at second order. The EDQNM yields equations for quadratic correlations (e.g., energies) expressed in terms of quadratic correlations. However, we take a simpler approach and apply the statistical ansatz of quasi-Gaussian statistics to the evolution equations directly, not the energies. The result is that the nonlinearities become turbulent diffusivities that depend on quadratic correlations and leave out incoherent and inhomogeneous forcing. This procedure does not correctly account for the energy balance of turbulence; however, it captures well the nonlinear decorrelation response at least dimensionally, by the renormalization of the turbulent response. This method was used in the investigation of flow shear suppression in neutral fluid¹⁵ and magnetic field shear suppression in kinetic Alfvén turbulence.¹⁸

We calculate the turbulent responses for the EDQNM procedure, obtaining the form $\tilde{L}_{ij}\Phi_j = S_i$, where $\Phi = (\tilde{\omega}, \tilde{j})$

$$\underbrace{\left(\gamma + i\Omega_\phi + d_{11} \frac{\partial^2}{\partial r^2} \right)}_{\tilde{L}_{11}} \tilde{\omega}_{km} + \underbrace{\left(-i\Omega_\psi + d_{12} \frac{\partial^2}{\partial r^2} \right)}_{\tilde{L}_{12}} \tilde{j}_{km} = -\frac{im}{r} \tilde{\phi} \frac{d\tilde{\omega}}{dr} + \frac{im}{r} \tilde{\psi} \frac{d\tilde{j}}{dr}, \quad (7a)$$

$$\underbrace{\left(-i\Omega_\psi + d_{21} \frac{\partial^2}{\partial r^2} \right)}_{\tilde{L}_{21}} \tilde{\omega}_{km} + \underbrace{\left(\gamma + i\Omega_\phi + d_{22} \frac{\partial^2}{\partial r^2} \right)}_{\tilde{L}_{22}} \tilde{j}_{km} = 0, \quad (7b)$$

where only the highest-order radial derivative terms are retained consistent with standard asymptotic boundary layer analysis for large shear in the magnetic field and flow (the detailed procedure is shown in Appendix A). The nonlinear diffusion coefficients are nominally all the same order of $d_{ij} \sim d$, where d indicates $O(d_{ij})$, which complicates the analysis. The Laplace transform is applied to the fast-time fluctuation. The radial derivatives of the slowly evolving (and dominant) current and vorticity in the right-hand side represent forcing or damping terms proportional to gradient. Each nonlinear diffusion coefficients d_{ij} has contributions from magnetic field and velocity field correlations

$$d_{ij} = d_{\phi\phi}^{ij} + d_{\phi\psi}^{ij} + d_{\psi\phi}^{ij} + d_{\psi\psi}^{ij},$$

where $d_{\alpha\beta}^{ij}$ are defined in Eqs. (A7)–(A10) with $\alpha, \beta = (\phi, \psi)$. As an example, the coefficient $d_{\phi\phi}^{11}$ is given by

$$d_{\phi\phi}^{11} = -\frac{1}{2\pi i} \int_{-i\infty+\gamma}^{i\infty+\gamma_0} d\gamma' \frac{im'}{r} \phi_{m',\gamma'} \left(\frac{\tilde{L}_{22}}{\text{Det}(\tilde{L}_{ij})} \right) W_{\gamma',\gamma'} \times \left(\frac{-im'}{r} \right) \phi_{-m',-\gamma'}, \quad (8)$$

where $W_{\gamma',\gamma'}$ is the decorrelation rate for fluctuations at γ' driving γ , and $\text{Det}(\tilde{L}_{ij}) = \tilde{L}_{11}\tilde{L}_{22} - \tilde{L}_{12}\tilde{L}_{21}$. Equation (8) implies that a radial velocity fluctuation $\tilde{v}_r = (-im'/r)\phi_{-m',-\gamma'}$ of a poloidal wavenumber $-m'$ is propagated by the response function $\tilde{L}_{22}/(\tilde{L}_{11}\tilde{L}_{22} - \tilde{L}_{12}\tilde{L}_{21})$ and interacts with the radial velocity fluctuation $\tilde{v}_r = (im'/r)\phi_{m',\gamma'}$ of the poloidal

wavenumber m' giving rise to nonlinear diffusion. The closure equations are renormalized by replacing the linear response function by \tilde{L}_{ij} in the nonlinear diffusion coefficients d_{ij} . There are sixteen $d_{\alpha\beta}^{ij}$, $2(\alpha = \tilde{\phi}, \tilde{\psi}) \times 4(\tilde{L}_{ij}/\text{Det}(\tilde{L}_{ij})) \times 2$ ($\beta = \tilde{\phi}, \tilde{\psi}$). The derivation and the detailed definition of d_{ij} are presented in Appendix A.

The nonlinear diffusion d_{ij} is generally complex. When it is real, such as in strong turbulence of Navier-Stokes and MHD systems, the nonlinear interaction described by d_{ij} can be simply modeled as eddy damping. Therefore, the diagonal components, d_{11} and d_{22} , represent generalized turbulent viscosity and resistivity. The non-diagonal components, d_{12} and d_{21} , describe the modification to wave dynamics by nonlinear interactions between velocity field and magnetic field. In comparing Eqs. (4a) and (4b) with Eqs. (7a) and (7b) we observe that the nonlinearities have been replaced with $d_{11}\partial^2/\partial r^2$, $d_{12}\partial^2/\partial r^2$, $d_{21}\partial^2/\partial r^2$, and $d_{22}\partial^2/\partial r^2$. Thus we expect that the radial correlation lengths will involve ratios of d_{ij}/Ω' . The diffusivities are proportional to quadratic correlations of fluctuation levels and account for how the fluctuations interact dynamically to give rise to decorrelation. Dimensionally the diffusivities are proportional quadratically to fluctuations in the weak turbulence regime, i.e., $d_{\phi\phi} \sim \tilde{\phi}^2$; in the strong turbulence regime the diffusivities vary linearly, i.e., $d_{\phi\phi} \sim \phi$.

A more complete closure would also determine the incoherent turbulent source and satisfy other constraints, such as realizability.²⁴ However, because shearing is a linear process in the two time scale analysis, its effect on turbulence correlations and levels resides in the turbulent response, making the present treatment adequate. We also note that, like the description of coherent vortices in 2D Navier-Stokes turbulence,¹⁵ the two time scale analysis separates the coherent, non-Gaussian component of turbulence (in this case the dominant helicity mode) from the incoherent Gaussian component (other helicities), justifying the quasi-Gaussian approximation of the closure.

III. SCALING OF TURBULENT BOUNDARY LAYER

Solving Eqs. (7a) and (7b) is a highly difficult task, if possible. Rather than seeking a solution, a response function for turbulent fluctuations can be explored by asymptotic expansion for large shear. The response functions $G_{\tilde{\omega}}$ and $G_{\tilde{j}}$ of vorticity and current perturbations $\tilde{\omega}$ and \tilde{j} satisfy

$$\begin{aligned} \tilde{L}_{11}G_{\tilde{\omega}}(r, r') + \tilde{L}_{12}G_{\tilde{j}}(r, r') &= \delta(r - r'), \\ \tilde{L}_{21}G_{\tilde{\omega}}(r, r') + \tilde{L}_{22}G_{\tilde{j}}(r, r') &= 0. \end{aligned} \tag{9}$$

When the equations are solved for $G_{\tilde{\omega}, \tilde{j}}$, turbulent fluctuations $\tilde{\omega}$ and \tilde{j} are

$$(\tilde{\omega}, \tilde{j}) = \int_{r'} G_{\tilde{\omega}, \tilde{j}}(r, r')R(r'),$$

where R represents the inhomogeneous terms in Eqs. (7a) and (7b). Since large shear results in a sharp decrease in turbulent fluctuations over a short radial distance, the WKB expansion is best suited for the problems.²⁵ The WKB ansatz yields

$$G_{\tilde{\omega}} = \exp\left(\sum_{n=-n_{\tilde{\omega}}} \epsilon^n S_{\tilde{\omega}, n}\right) \quad \text{and} \quad G_{\tilde{j}} = \exp\left(\sum_{n=-n_{\tilde{j}}} \epsilon^n S_{\tilde{j}, n}\right),$$

where ϵ is an order parameter. A complex function $S(r, r')$ represents both amplitude and phase change from the source $R(r')$. If $G \sim \exp(-|r - r_0|^n/S_0)$, the fluctuation falls off exponentially over a boundary layer width $\Delta r = |r - r'| = S_0^{1/n}$, where $|G(\Delta r)| = 1/e$. The formal procedure for G is to obtain $G^+(r > r')$ and $G^-(r > r')$ and match asymptotically over $r = r'$. However, the solutions for the homogeneous equation (9) is enough for the investigation of the boundary layer width Δr . In addition, the turbulent diffusion d is treated as a given characteristic of turbulence existing outside the dominant helical structure.

It is assumed that the ratio of shear to diffusion is proportional to $1/\epsilon^2$ where $\Omega'_\phi, \Omega'_\psi \sim 1/\epsilon^2$ where ϵ is small. That limit corresponds to $\max(\Omega'_\psi, \Omega'_\phi)\Delta r/d \sim O(\epsilon^{-2}) \gg 1$. The solutions can be sought for with $n_{\tilde{\omega}} = n_{\tilde{j}} = -1$. Therefore, we insert the first and second derivatives

$$\begin{aligned} \frac{\partial G_{\tilde{\omega}}}{\partial r} &\sim \epsilon^{-1} \frac{\partial S_{\omega, -1}}{\partial r} G_{\tilde{\omega}} \quad \text{and} \\ \frac{\partial^2 G_{\tilde{\omega}}}{\partial r^2} &\sim \epsilon^{-2} \left(\frac{\partial S_{\omega, -1}}{\partial r}\right)^2 G_{\tilde{\omega}} \end{aligned}$$

into Eq. (9). Analytical solution is possible with the assumptions of $\gamma + i\Omega_\phi$ and $k + i\Omega_\psi$ being in the smaller order than $1/\epsilon^2$ and $G_{\tilde{\omega}} = cG_{\tilde{j}}$, where c is a complex constant. The exponent $S_{\omega, -1} \sim r\sqrt{r}$ is obtained. Then the boundary layer width Δr over which fluctuations decrease exponentially is

$$\left(\frac{1}{\Delta r}\right)^3 \sim -i \frac{\Omega'_\psi(d_{12} + d_{21}) + \Omega'_\phi(d_{11} + d_{22})}{2\text{Det}(d_{ij})} - i \sqrt{\frac{[\Omega'_\psi(d_{12} + d_{21}) + \Omega'_\phi(d_{11} + d_{22})]^2 + 4\text{Det}(d_{ij})(\Omega_\phi'^2 - \Omega_\psi'^2)}{2\text{Det}(d_{ij})}}. \tag{10}$$

Here the expression (10) is obtained with $c = 1$. Notice that d_{ij} is complex and so is Δr . Due to complex Δr , the fluctuation which penetrates into the dominant mode is oscillatory in general. Still, Δr is a good measure of the length scale over which fluctuations decrease significantly.

The dominant radial scale (turbulent boundary layer width) can be divided into two limiting cases. One is the

“linear” interaction between flow and magnetic shears resulting when $Q \gg 1$ where

$$Q \equiv \left| \frac{[\Omega'_\psi(d_{12} + d_{21}) + \Omega'_\phi(d_{11} + d_{22})]^2}{4\text{Det}(d_{ij})(\Omega_\phi'^2 - \Omega_\psi'^2)} \right|, \tag{11}$$

where Q is simply the ratio of the first term to the second one in the radical of Eq. (10). Here, “linear” simply mean that the effective shear Ω'_{eff} can be expressed a linear combination of magnetic and flow shears, as $\Omega'_{\text{eff}} = c_1(\Omega'_\phi + c_2\Omega'_\psi)$ where $c_{1,2}$ are complex constants, or

$$\left(\frac{1}{\Delta r}\right)^3 \sim -i \frac{\Omega'_\psi(d_{12} + d_{21}) + \Omega'_\phi(d_{11} + d_{22})}{\text{Det}(d_{ij})}. \quad (12)$$

The signs of $\text{Re } c_1$ and $\text{Re } c_2$ are dependent on the nonlinear diffusion coefficients d_{ij} , which are determined by the correlations of the turbulent magnetic field and velocity fluctuations outside the dominant mode structure. We do not go into the details of Alfvénic turbulence, related to overlapping tearing modes. Since flow shear is well-known to suppress turbulence in general, we start with an assumption that $\text{Re } c_1 > 0$. Then, magnetic shear suppresses the turbulence together with flow shear if $\text{Re } c_2 > 0$. Magnetic shear weakens the suppression by flow if $\text{Re } c_2 < 0$. And in this case, the relative direction of each shear is important.

In the other limiting case $Q \ll 1$, the effective shear can be expressed in the quadratic relation between magnetic and flow shears, $\Omega'_{\text{eff}} = c_3 \sqrt{\Omega_\phi'^2 - \Omega_\psi'^2}$. The magnetic shear and the flow shear always cancel out so as to weaken the suppression. The “quadratic” interaction is independent of the ambient turbulence since the effective shear is proportional to $\Omega_\phi'^2 - \Omega_\psi'^2$ in comparison to $\Omega'_\phi + c_2\Omega'_\psi$, where c_2 is dependent on turbulent fluctuations. In this case

$$\left(\frac{1}{\Delta r}\right)^3 \sim -i \sqrt{\frac{\Omega_\phi'^2 - \Omega_\psi'^2}{\text{Det}(d_{ij})}}. \quad (13)$$

In fact, the division of “linear” and “quadratic” interactions between the shears is somewhat artificial, and the boundary layer widths for both interactions have the same scaling of

$$\Delta r \sim \left(\frac{d}{\Omega'_{\text{eff}}}\right)^{1/3}, \quad (14)$$

where a generic d represents nonlinear diffusion d_{ij} for scaling analysis. However, the distinction between “linear” and “quadratic” interactions is instructive when $Q \gg (\ll) 1$.

In order to make clear the relation between magnetic shear and flow shear, it is helpful to take a quasilinear approximation. In the quasilinear limit, the linear operators L_{ij} without nonlinear diffusion coefficients d_{ij} , instead of the renormalized operators \tilde{L}_{ij} , are used for the calculation of the nonlinear diffusion coefficients d_{ij} as shown in Appendix B. Since $L_1 \equiv L_{11} = L_{22}$ and $L_2 \equiv L_{12} = L_{21}$, there are only two propagators of $P_\pm = 1/(L_1 \mp L_2)$ in comparison to the four nonlinear propagator $\tilde{L}_{ij}/\text{Det}(\tilde{L}_{ij})$ in Eq. (8). Two propagators P_\pm correspond to the Alfvén waves propagating forward and backward along the magnetic field line of the dominant mode. Then the nonlinear diffusion coefficients d_{ij} are expressed in the linear combination of eight nonlinear decorrelation rates $d_{\alpha\beta}^{(\ell)\pm}$ ($2 \times 2 \times 2$), where α, β being $(\tilde{\phi}, \tilde{\psi})$ (refer to Eq. (B2)). Here the superscript (ℓ) are used for the quasilinear decorrelation rates to avoid confusion: $d_{\phi\phi}^{(\ell)+}$ is the quasilinear diffusion coefficient arising from the interaction of electrostatic fluctua-

tions, i.e., velocity fluctuations. In the case where the wave turbulence is well balanced between the waves propagating in both the directions, that is, $d_{\alpha\beta}^{(\ell)} \equiv d_{\alpha\beta}^{(\ell)+} = d_{\alpha\beta}^{(\ell)-}$, the boundary width of the “linear” interaction can be simplified

$$\left(\frac{1}{\Delta r}\right)^3 \sim -i \frac{d_{\phi\phi}^{(\ell)}\Omega'_\phi - d_{\phi\psi}^{(\ell)}\Omega'_\psi}{\text{Det}(d_{ij}^{(\ell)})}, \quad (15)$$

where $\text{Det}(d_{ij}^{(\ell)}) = (d_{\phi\phi}^{(\ell)} - d_{\psi\psi}^{(\ell)}) - (d_{\phi\psi}^{(\ell)} - d_{\psi\phi}^{(\ell)})$. The width of the “quadratic” interaction is the same as Eq. (13) except the new determinant. Now Eq. (15) shows when flow shear dominates magnetic shear in the “linear” interaction. Consider that both shears are the same order of amplitude. When the decorrelation arising from the nonlinear interactions between velocity fluctuations or magnetic field fluctuations are large in comparison to the one arising between velocity and magnetic field fluctuations, i.e., $d_{\phi\phi}^{(\ell)}, d_{\psi\psi}^{(\ell)} \gg d_{\phi\psi}^{(\ell)}, d_{\psi\phi}^{(\ell)}$, the flow shear mainly determines the effective shear and the turbulent boundary layer $(\Delta r)^{-3} \rightarrow \Omega'_\phi/d_{\phi\phi}^{(\ell)}$. When $d_{\phi\phi}^{(\ell)}, d_{\psi\psi}^{(\ell)} \ll d_{\phi\psi}^{(\ell)}, d_{\psi\phi}^{(\ell)}$, the magnetic field shear makes a larger contribution to the effective shear and the boundary width dominantly, yielding $(\Delta r)^{-3} \rightarrow \Omega'_\psi/d_{\phi\psi}^{(\ell)}$.

The interaction between magnetic shear and flow is shown to be dependent on the turbulent correlations. Although d_{ij} is likely to be in the same order, the above description of either linear or quadratic shear-shear interactions allows better insight into the relation of shear strengths. In the “linear” interaction between the two shears, the scaling can be written with the Alfvén velocity $V_A(r_0)$ and flow velocity $V_0(r_0)$ of the dominant mode

$$\frac{1}{(\Delta r)^3} \sim \frac{(\Omega'_\phi + \alpha\Omega'_\psi)}{d} \sim \frac{1}{d} \frac{d}{dr} \left(\frac{B_\theta}{r}\right) \left(\frac{V_0 L_J}{V_A L_\Omega} + \alpha\right), \quad (16)$$

where the coefficient α is in general $\sim O(1)$, the flow shear length $L_\Omega = \Omega_\phi/\Omega_{\phi'}$, and the field shear length $L_J = \Omega_\phi/\Omega_{\phi'}$. In case of the sub-Alfvénic flow ($V_A/V_0 \ll 1$) and the similar shear lengths of flow and magnetic field, $L_J \sim L_\Omega$, a coherent structure is likely to be bounded by the magnetic field shear $\Omega'_\psi = r^{-1}d(B_\theta/r)/dr$, not by the flow shear $\Omega'_\phi = d(V_0/r)/dr$.

IV. COMPARISON TO TEARING MODES

In Sec. III, from the structure of the dominant mode, the scaling of the turbulent boundary layer width Δr is obtained in terms of the magnetic and flow shears and the turbulent diffusion rates. A condition for the existence of a single helical state will be developed in this section.

The local approximation is valid when the boundary layer width is far smaller than the magnetic scale length ℓ_J , or flow shear length ℓ_Ω . For this to hold, the boundary width Δr should satisfy

$$\frac{\Delta r}{\min(\ell_J, \ell_\Omega)} \ll 1.$$

In addition, for the effective suppression, a boundary layer should be smaller than any macroscopic length associated

with fluctuations outside the layer. The magnetic island width w_0 , formed by an unstable tearing mode, is the smallest of the macroscopic length scales. The island width should be larger than the width of the boundary layer so that the island structure serves as a coherent structure in this context. The criterion for the turbulence suppression, then, becomes

$$\Delta r/w_0 \ll 1. \quad (17)$$

The width of the nonlinear tearing mode is $w_0 \sim \sqrt{r q B_r^{\text{tearing}}/m q' B_\theta^{\text{eq}}}$ [chap. 7.2 of Wesson²⁶] where B_r^{tearing} is the radial magnetic field of a tearing mode, B_θ^{eq} is the poloidal magnetic field of the equilibrium, and q is the safety factor. When the helical structure of a tearing mode is to be treated as the dominant fluctuation structure described in Sec. II, the magnetic field associated with the magnetic shear should be orthogonal to both the radial direction and the mode propagation directions of the tearing modes. In this orthogonal direction, the local magnetic shear Ω'_ψ of the coherent structure is not the same as the equilibrium magnetic field B_θ^{eq} giving rise to unstable tearing modes. The tearing mode forms a resonant surface that is helical in nature. A perturbation resonant with this resonant surface has the form of $\exp(im\chi)$, where $\chi = \theta - (n/m)\phi$ is an angular coordinate orthogonal to the helix. The magnetic field in this orthogonal direction is

$$\bar{B}^* = B_\theta^{\text{eq}} \left(1 - \frac{n}{m} q(r)\right) = -\left(\frac{q' B_\theta^{\text{eq}}}{q}\right) (r - r_s), \quad (18)$$

where r_s is the resonant surface $q(r_s) = m/n$.

The local magnetic field shear experienced by the turbulence is from \bar{B}^* , not from B_θ^{eq} . The angular Alfvén velocity Ω_ψ arises from $\bar{B}^*/r \sim q' B_\theta^{\text{eq}}/q$.

Therefore, the qualitative comparison gives the maximal suppression for

$$\frac{\Delta r}{w_0} \sim \left| \frac{d^{1/3}}{\Omega_{\text{eff}}^{1/3}} \left(\frac{\Omega_\psi}{B_r^{\text{tearing}}} \right)^{1/2} \right| \ll 1. \quad (19)$$

From a naive observation, the magnetic shear from q' in the magnetic island width would weaken the effect of the magnetic shear in Ω_{eff} , leading to a less optimal condition for magnetic shear suppression. However, the macro shear q' only increases the angular frequency Ω_ψ of the local tearing magnetic field, giving equal footing to both local magnetic and flow shear from the unstable tearing modes. As far as the ratio of a turbulent boundary width to a magnetic island width is concerned, it does not matter whether the effective shear is from the magnetic field or the flow shear.

Vortex structures decay as a result of turbulence mixing as shown in the RHS of Eq. (3). In Eq. (7), it is possible to estimate \tilde{L}_{ij} dimensionally, i.e., $\tilde{L}_{11} \sim (\Omega'_\psi + d_{11}/\Delta r^3)r$. The rate of mixing is governed by the amplitude of turbulent fluctuations in the layer. The fluctuation amplitudes $\hat{\omega}$ and \hat{j} in the vortex could be algebraically estimated with $r \sim \Delta r$

$$\begin{aligned} \hat{\omega} &\sim \frac{\Omega'_\phi + d_{22}/\Delta r^3}{\Omega_{\text{eff}}^2 \Delta r} \frac{im}{r} \left(\tilde{\psi} \frac{d\bar{j}}{dr} - \tilde{\phi} \frac{d\bar{\omega}}{dr} \right), \\ \hat{j} &\sim \frac{\Omega'_\psi + d_{21}/\Delta r^3}{\Omega_{\text{eff}}^2 \Delta r} \frac{im}{r} \left(\tilde{\psi} \frac{d\bar{j}}{dr} - \tilde{\phi} \frac{d\bar{\omega}}{dr} \right). \end{aligned}$$

Both fluctuation levels in the coherent structure are inversely proportional to $\Omega_{\text{eff}}' \Delta r$ since $\Omega'_\psi, \Omega'_\phi, d_{ij}/\Delta r^3 \sim \Omega_{\text{eff}}'$. This factor reduces the levels and makes the fluctuations much less efficient at relaxing the coherent structure profiles via turbulent diffusion. The profile relaxation times are denoted by $\tau_{\bar{\omega}}$ and $\tau_{\bar{j}}$, and their magnitudes can be extracted dimensionally from the following:

$$\begin{aligned} \frac{\bar{\omega}}{\tau_{\bar{\omega}}} &\sim -\frac{1}{2\pi i} \int d\gamma \left\langle -\sum_{k', m'} \left[\frac{im'}{r} \left(\frac{\partial \tilde{\phi}'^*}{\partial r} \bar{\omega}' - \frac{\partial \bar{\omega}'^*}{\partial r} \tilde{\phi}' \right) \right. \right. \\ &\quad \left. \left. - \frac{im'}{r} \left(\frac{\partial \tilde{\psi}'^*}{\partial r} \bar{j}' - \frac{\partial \bar{j}'^*}{\partial r} \tilde{\psi}' \right) \right] \right\rangle \\ &\sim \frac{1}{\Omega_{\text{eff}}'^2 \Delta r^3} \left[(\langle b_r v_r \rangle - \langle v_r b_r \rangle) \frac{d\bar{\omega}}{dr} + (\langle v_r b_r \rangle - \langle b_r b_r \rangle) \frac{d\bar{j}}{dr} \right], \end{aligned}$$

where $\partial/\partial r \sim 1/\Delta r$ and $\int d\gamma \langle \tilde{\phi} \tilde{\psi} \rangle \sim \tilde{\phi} \tilde{\psi} / \Omega_{\text{eff}}' \Delta r$ are used. Assuming $\langle v_r v_r \rangle \sim \langle v_r b_r \rangle \sim \langle b_r b_r \rangle$ and strong turbulence $d \sim b_r$, the estimate $\tau_{\bar{\omega}} \sim \tau_{\bar{j}}$ is

$$\frac{1}{\tau_{\bar{j}}} \sim \frac{1}{\tau_{\bar{\omega}}} \sim \frac{b_r}{\Omega_{\text{eff}}'} \sim \frac{b_r}{q' B_\theta^{\text{eq}} / (q \ell_B)} \sim \frac{b_r}{B_\theta^{\text{eq}}} \frac{\ell_B}{q}. \quad (20)$$

The life time of the vortex structure is proportional to the effective shear Ω_{eff}' , which, for the RFP equilibrium, can be represented by B_θ^{eq}/b_r .

If the shearing effects described here are excluded, the coherent structure is an unstable tearing mode with a linear growing rate $\gamma_{\text{tearing}} = \tau_{\text{tearing}}^{-1}$. This time scales parametrizes not just instability, but nonlinear saturation. Hence a comparison of $\tau_{\bar{j}}$ with τ_{tearing} indicates the extent to which shearing effects modify the dynamics. When $\tau_{\bar{j}}/\tau_{\text{tearing}} \geq 1$, the innermost tearing mode can sustain itself by suppressing the incoming turbulence generated by other outlying tearing modes. Assuming that all radial derivatives, q'/q and ℓ_B , are all tied to the poloidal magnetic field B_θ , we compare the life time $\tau_{\bar{j}}$ to the linear tearing growth rates. For the sake of comparison we consider the behavior of $\gamma_{\text{tearing}} \tau_{\bar{j}}$ for a tokamak. For the tokamak, the linear growth rate is $\gamma_{\text{tearing}} \sim (q')^{2/3} \tau_R^{1/3} \tau_A^{2/3} \sim B_\theta^{-2/3}$ for $m=1$.²⁷

$$\gamma_{\text{tearing}} \tau_{\bar{j}} \sim B_\theta^{1/3} (\text{Tokamak}).$$

For larger poloidal magnetic field, the ratio of structure life-time to tearing mode growth time is larger. For the RFP, the linear tearing growth rate is $\gamma_{\text{tearing}}(\text{RFP}) \sim B_\theta^{2/5}$.²⁸ Since the poloidal magnetic field and the toroidal magnetic field in the RFP are of the same order, the linear growth rate should be proportional to a power of the poloidal magnetic field between 0 and 2/5. This yields

$$\gamma_{\text{tearing}} \tau_{\bar{j}} \sim B_\theta^\alpha (\text{RFP}),$$

where $1 < \alpha < 1.4$. We observe that the scaling of lifetime with B_θ is much stronger (more favorable for coherence) in the RFP than in the tokamak.

This result is qualitatively consistent with the observation of the longer persistence of the QSH state with the increase of plasma current.²⁹ Since the resistivity and the viscosity are not included in the analysis, it is hard to directly compare our result to the Lundquist number scaling²⁹ with the amplitudes of the dominant mode and secondary modes, where the amplitude of the dominant mode increases with the Lundquist number and the amplitudes of the secondary modes decrease. The decrease of the amplitudes of the secondary modes, whatever its reason, is more likely to enhance the shear suppression by these shears, since the secondary modes are the source of free energy for the turbulence represented by d in the scaling.

V. CONCLUSION

We have obtained the scaling for the turbulent boundary width established in the presence of the large magnetic and velocity shears of a coherent vortex structure, based on the fact that either large flow shear or magnetic shear suppresses turbulence unless there is instability induced by one of shears. The turbulent layer width is inversely proportional to an effective shear $\Omega_{\text{eff}}^{1/3}$, where the effective shear is a dimensional estimate extracted from the combination of complicated nonlinear diffusions and the magnetic and flow shears. The effective shear is characterized in two limits as having either a “linear” or “quadratic” interaction between the magnetic and flow shears. In the “linear” interaction, flow and magnetic field shears can suppress the ambient turbulence together or partially cancel each other to weaken nonlinear suppression depending on the relative direction of the shears. The characteristics of the ambient turbulence are important in deciding the relative roles of the shears. In the “quadratic” interaction, they always work against each other to weaken the nonlinear suppression. In the quasilinear approximation where the turbulent response is dominated by Alfvén waves, either of the shears is dominant in suppression and the other shear weakens the suppression by the “quadratic” interaction. Even though this paper does not explore a concrete relation between the shears in details, the result encompasses a large range of possibilities that can arise from the combination of magnetic and flow shears. Regardless of whether the system is in the linear or quadratic limit, system responses scale with $\Omega_{\text{eff}}^{1/3}$ with additive or subtractive combinations providing a larger or smaller overall numerical coefficient.

The scalings of the boundary layer width and the lifetime scaling of the coherent vortex structure are compared to the tearing island width and linear tearing growth rate, which quantifies the energy injection rate by tearing modes into the magnetic island. Larger shears give a longer life-time to the coherent structure in proportion to Ω_{eff} . A larger poloidal magnetic field tends to give a longer life-time. The life-time relative to the linear tearing growth time gives a stronger dependence on poloidal magnetic field in the RFP than in tokamaks, thus favoring the formation of this coherent structure

in the RFP. This is consistent with the observation that a helical state in the RFP is favored by large plasma current.

This dimensional analysis is based on the simple concept of the turbulent boundary layer. This analysis makes use of several simplifying assumptions. Account is not taken of a possible oscillatory response across the layer. The turbulence diffusion coefficients d_{ij} are treated independent of magnetic and flow shear. The coherent structure is treated as axisymmetric when in fact it is helical and three-dimensional. Quantitative results from numerical simulation are therefore highly desirable and will be pursued in the future. Despite the limitations of the approach, the trends represented by the scaling reflect robust physics and suggest new measurements. These include the magnetic shear and flow shear of the dominant helical state and turbulence inside and outside the helical structure.

ACKNOWLEDGMENTS

This work is supported by the U.S. Department of Energy (DOE) DE-SC0002322 under the Center for Momentum Transport and Flow Organization (CMTFO).

APPENDIX A: DERIVATION OF TURBULENT DIFFUSION COEFFICIENTS

In order to obtain the governing nonlinear equation, the set of the equations (4) is rewritten as

$$L_{11}\tilde{\omega} + L_{12}\tilde{j} = - \sum_{\substack{m'+m''=m \\ k'+k''=k}}^* \left[\frac{im'}{r} \left(\frac{\partial \tilde{\phi}''}{\partial r} \tilde{\omega}' - \frac{\partial \tilde{\omega}''}{\partial r} \tilde{\phi}' \right) - \frac{im'}{r} \left(\frac{\partial \tilde{\psi}''}{\partial r} \tilde{j}' - \frac{\partial \tilde{j}''}{\partial r} \tilde{\psi}' \right) \right], \quad (\text{A1a})$$

$$L_{21}\tilde{\phi} + L_{22}\tilde{\psi} = \sum_{\substack{m'+m''=m \\ k'+k''=k}}^* \frac{im'}{r} \left(\frac{\partial \tilde{\psi}''}{\partial r} \tilde{\phi}' - \frac{\partial \tilde{\phi}''}{\partial r} \tilde{\psi}' \right), \quad (\text{A1b})$$

where

$$L_1 = L_{11} = L_{22} = \frac{\partial}{\partial t} + \frac{im}{r} \frac{d\bar{\phi}}{dr} = \gamma + im\Omega_\phi(r), \quad (\text{A2})$$

$$L_2 = L_{12} = L_{21} = ik - \frac{im}{r} \frac{d\bar{\psi}}{dr} = i(k - m\Omega_\psi(r)).$$

Applying the Laplacian to Eq. (A1b) and dropping the lower derivative in Eq. (A1), we obtain

$$L_{11}\tilde{\omega} + L_{12}\tilde{j} = \sum_{\substack{m'+m''=m \\ k'+k''=k}}^* \frac{im'}{r} \left(\frac{\partial \tilde{\omega}''}{\partial r} \tilde{\phi}' - \frac{\partial \tilde{j}''}{\partial r} \tilde{\psi}' \right), \quad (\text{A3})$$

$$L_{21}\tilde{\omega} + L_{22}\tilde{j} = \sum_{\substack{m'+m''=m \\ k'+k''=k}}^* \frac{im'}{r} \left(\frac{\partial \tilde{j}''}{\partial r} \tilde{\phi}' - \frac{\partial \tilde{\omega}''}{\partial r} \tilde{\psi}' \right).$$

Then dropping the sum for simple notation yields

$$\begin{aligned} \tilde{\omega} &= \frac{1}{D_L} \left[\frac{im'}{r} L_{22} \left(\frac{\partial \tilde{\omega}''}{\partial r} \tilde{\phi}' - \frac{\partial \tilde{j}''}{\partial r} \tilde{\psi}' \right) - \frac{im'}{r} L_{12} \left(\frac{\partial \tilde{j}''}{\partial r} \tilde{\phi}' - \frac{\partial \tilde{\omega}''}{\partial r} \tilde{\psi}' \right) \right], \\ \tilde{j} &= \frac{1}{D_L} \left[-\frac{im'}{r} L_{21} \left(\frac{\partial \tilde{\omega}''}{\partial r} \tilde{\phi}' - \frac{\partial \tilde{j}''}{\partial r} \tilde{\psi}' \right) + \frac{im'}{r} L_{11} \left(\frac{\partial \tilde{j}''}{\partial r} \tilde{\phi}' - \frac{\partial \tilde{\omega}''}{\partial r} \tilde{\psi}' \right) \right], \end{aligned} \tag{A4}$$

where

$$D_L = L_{11}L_{22} - L_{12}L_{21}.$$

Substituting Eq. (A4) in the RHS of Eq. (A3), we obtain

$$\begin{aligned} \left(L_{11} + d_{11} \frac{\partial^2}{\partial r^2} \right) \tilde{\omega} + \left(L_{12} + d_{12} \frac{\partial^2}{\partial r^2} \right) \tilde{j} &= f, \\ \left(L_{21} + d_{21} \frac{\partial^2}{\partial r^2} \right) \tilde{\omega} + \left(L_{22} + d_{22} \frac{\partial^2}{\partial r^2} \right) \tilde{j} &= g, \end{aligned} \tag{A5}$$

where f, g are the source terms independent of $\hat{\omega}$ and \hat{j}

$$d_{ij} = d_{\phi\phi}^{ij} + d_{\phi\psi}^{ij} + d_{\psi\phi}^{ij} + d_{\psi\psi}^{ij}, \tag{A6}$$

i and j are the indexes of $\{1, 2\}$, and

$$\begin{aligned} d_{\phi\phi}^{11} &= \left\langle \left(\frac{im'}{r} \tilde{\phi}' \right) \frac{L_{22}}{D_L} \left(\frac{-im'}{r} \tilde{\phi}_{-m'} \right) \right\rangle, \\ d_{\phi\psi}^{11} &= \left\langle \left(\frac{im'}{r} \tilde{\phi}' \right) \frac{L_{12}}{D_L} \left(\frac{-im'}{r} \tilde{\psi}_{-m'} \right) \right\rangle, \\ d_{\psi\phi}^{11} &= \left\langle -\left(\frac{im'}{r} \tilde{\psi}' \right) \frac{L_{21}}{D_L} \left(\frac{-im'}{r} \tilde{\phi}_{-m'} \right) \right\rangle, \\ d_{\psi\psi}^{11} &= \left\langle -\left(\frac{im'}{r} \tilde{\psi}' \right) \frac{L_{11}}{D_L} \left(\frac{-im'}{r} \tilde{\psi}_{-m'} \right) \right\rangle, \end{aligned} \tag{A7}$$

$$\begin{aligned} d_{\phi\phi}^{12} &= \left\langle -\left(\frac{im'}{r} \tilde{\phi}' \right) \frac{L_{12}}{D_L} \left(\frac{-im'}{r} \tilde{\phi}_{-m'} \right) \right\rangle, \\ d_{\phi\psi}^{12} &= \left\langle -\left(\frac{im'}{r} \tilde{\phi}' \right) \frac{L_{22}}{D_L} \left(\frac{-im'}{r} \tilde{\psi}_{-m'} \right) \right\rangle, \\ d_{\psi\phi}^{12} &= \left\langle \left(\frac{im'}{r} \tilde{\psi}' \right) \frac{L_{11}}{D_L} \left(\frac{-im'}{r} \tilde{\phi}_{-m'} \right) \right\rangle, \\ d_{\psi\psi}^{12} &= \left\langle \left(\frac{im'}{r} \tilde{\psi}' \right) \frac{L_{21}}{D_L} \left(\frac{-im'}{r} \tilde{\psi}_{-m'} \right) \right\rangle, \end{aligned} \tag{A8}$$

$$\begin{aligned} d_{\phi\phi}^{21} &= \left\langle -\left(\frac{im'}{r} \tilde{\phi}' \right) \frac{L_{21}}{D_L} \left(\frac{-im'}{r} \tilde{\phi}_{-m'} \right) \right\rangle, \\ d_{\phi\psi}^{21} &= \left\langle -\left(\frac{im'}{r} \tilde{\phi}' \right) \frac{L_{11}}{D_L} \left(\frac{-im'}{r} \tilde{\psi}_{-m'} \right) \right\rangle, \\ d_{\psi\phi}^{21} &= \left\langle -\left(\frac{im'}{r} \tilde{\psi}' \right) \frac{L_{22}}{D_L} \left(\frac{-im'}{r} \tilde{\phi}_{-m'} \right) \right\rangle, \\ d_{\psi\psi}^{21} &= \left\langle -\left(\frac{im'}{r} \tilde{\psi}' \right) \frac{L_{12}}{D_L} \left(\frac{-im'}{r} \tilde{\psi}_{-m'} \right) \right\rangle, \end{aligned} \tag{A9}$$

$$\begin{aligned} d_{\phi\phi}^{22} &= \left\langle \left(\frac{im'}{r} \tilde{\phi}' \right) \frac{L_{11}}{D_L} \left(\frac{-im'}{r} \tilde{\phi}_{-m'} \right) \right\rangle, \\ d_{\phi\psi}^{22} &= \left\langle \left(\frac{im'}{r} \tilde{\phi}' \right) \frac{L_{21}}{D_L} \left(\frac{-im'}{r} \tilde{\psi}_{-m'} \right) \right\rangle, \\ d_{\psi\phi}^{22} &= \left\langle \left(\frac{im'}{r} \tilde{\psi}' \right) \frac{L_{12}}{D_L} \left(\frac{-im'}{r} \tilde{\phi}_{-m'} \right) \right\rangle, \\ d_{\psi\psi}^{22} &= \left\langle \left(\frac{im'}{r} \tilde{\psi}' \right) \frac{L_{22}}{D_L} \left(\frac{-im'}{r} \tilde{\psi}_{-m'} \right) \right\rangle. \end{aligned} \tag{A10}$$

In the above expressions the angle bracket $\langle \dots \rangle$ are a shorthand notation of

$$\langle \dots \rangle = \sum_{m'} \frac{1}{2\pi i} \int_{-i\infty+\gamma_0}^{i\infty+\gamma_0} W_{\gamma', \gamma'} d\gamma'(\dots), \tag{A11}$$

where $W_{\gamma', \gamma'}$ is the decorrelation rate for fluctuations at γ' driving γ . The diffusion coefficients d_{ij} in the Eqs. (A7)–(A10) is defined in terms of the linear operators L_{ij} .

From the renormalization procedure, it follows that the linear operators in the LHS of Eq. (A5) are redefined as

$$\tilde{L}_{ij} = L_{ij} + \tilde{d}_{ij} \frac{\partial^2}{\partial r^2} \tag{A12}$$

and \tilde{d}_{ij} is d_{ij} defined with \tilde{L}_{ij} instead of L_{ij} in Eqs. (A7)–(A10). For simplicity the tilde ($\tilde{}$) is dropped and d_{ij} is used for the renormalized nonlinear diffusion rates.

APPENDIX B: EDDY DAMPING RATE IN QUASILINEAR LIMIT

In the quasilinear limit where the nonlinear diffusion coefficients d_{ij} are determined by the linear response function L_{ij} without the renormalization, Eq. (A12), the shear interaction is transparent. In this zeroth order approximation of L_{ij} , using Eq. (A2),

$$D_L = L_1^2 - L_2^2 \tag{B1}$$

and

$$\begin{aligned} \frac{L_{11}}{D_L} &= \frac{L_{22}}{D_L} = \frac{L_1}{D_L} = P_+ + P_-, \\ \frac{L_{12}}{D_L} &= \frac{L_{21}}{D_L} = \frac{L_2}{D_L} = P_+ - P_-, \end{aligned}$$

where the forward and backward Alfvén propagators are

$$P_+ = \frac{1}{L_1 - L_2} \quad \text{and} \quad P_- = \frac{1}{L_1 + L_2}.$$

Each nonlinear diffusion d_{ij} can be written

$$\begin{aligned} 2d_{11} &= \left(d_{\phi\phi}^{(\ell)+} + d_{\phi\phi}^{(\ell)-}\right) + \left(d_{\phi\psi}^{(\ell)+} - d_{\phi\psi}^{(\ell)-}\right) - \left(d_{\psi\phi}^{(\ell)+} - d_{\psi\phi}^{(\ell)-}\right) - \left(d_{\psi\psi}^{(\ell)+} + d_{\psi\psi}^{(\ell)-}\right), \\ 2d_{12} &= -\left(d_{\phi\phi}^{(\ell)+} - d_{\phi\phi}^{(\ell)-}\right) - \left(d_{\phi\psi}^{(\ell)+} + d_{\phi\psi}^{(\ell)-}\right) + \left(d_{\psi\phi}^{(\ell)+} + d_{\psi\phi}^{(\ell)-}\right) + \left(d_{\psi\psi}^{(\ell)+} - d_{\psi\psi}^{(\ell)-}\right), \\ 2d_{21} &= -\left(d_{\phi\phi}^{(\ell)+} - d_{\phi\phi}^{(\ell)-}\right) - \left(d_{\phi\psi}^{(\ell)+} + d_{\phi\psi}^{(\ell)-}\right) - \left(d_{\psi\phi}^{(\ell)+} + d_{\psi\phi}^{(\ell)-}\right) - \left(d_{\psi\psi}^{(\ell)+} - d_{\psi\psi}^{(\ell)-}\right), \\ 2d_{22} &= \left(d_{\phi\phi}^{(\ell)+} + d_{\phi\phi}^{(\ell)-}\right) + \left(d_{\phi\psi}^{(\ell)+} - d_{\phi\psi}^{(\ell)-}\right) + \left(d_{\psi\phi}^{(\ell)+} - d_{\psi\phi}^{(\ell)-}\right) + \left(d_{\psi\psi}^{(\ell)+} + d_{\psi\psi}^{(\ell)-}\right), \end{aligned} \quad (\text{B2})$$

where

$$d_{\alpha\beta}^{(\ell)\pm} = \left\langle \left(\frac{im'}{r} \alpha' \right) P_{\pm} \left(\frac{-im'}{r} \beta_{-m'} \right) \right\rangle, \quad (\text{B3})$$

and α and β are either the electrostatic potential fluctuation ϕ or the magnetic flux fluctuation ψ .

- ¹P. Martin, L. Marrelli, G. Spizzo *et al.*, "Overview of quasi-single helicity experiments in reversed field pinches," *Nucl. Fusion* **43**, 1855 (2003).
- ²R. Lorenzini, D. Terranova, A. Alfieri, P. Innocente, E. Martinez, R. Pasqualotto, and P. Zanca, "Single-helical-axis states in reversed-field-pinch plasmas," *Phys. Rev. Lett.* **101**, 025005 (2008).
- ³R. Lorenzini, E. Martinez, P. Piovesan, D. Terranova, P. Zanca, M. Zuin, A. Alfieri, D. Bonfiglio, F. Bonomo, A. Canton, S. Cappello, L. Carraro, R. Cavazzana, D. F. Escande, A. Fassina, P. Franz, M. Gobbin, P. Innocente, L. Marrelli, R. Pasqualotto, M. E. Puiatti, M. Spolaore, M. Valisa, N. Vianello, and P. Martin, "Self-organized helical equilibria as a new paradigm for ohmically heated fusion plasmas," *Nat. Phys.* **5**, 570 (2009).
- ⁴B. E. Chapman, J. W. Ahn, A. F. Almagri, J. K. Anderson, F. Bonomo, D. Brower, D. Burke, K. Caspary, D. Clayton, S. Combs *et al.*, "Improved-confinement plasmas at high temperature and high beta in the MST RFP," *Nucl. Fusion* **49**, 104020 (2009).
- ⁵P. Martin, J. Adamek, P. Agostinetti *et al.*, "Overview of the RFX fusion science program," *Nucl. Fusion* **51**, 094023 (2011).
- ⁶D. F. Escande, R. Paccagnella, S. Cappello, C. Marchetto, and F. D'Angelo, "Chaos healing by separatrix disappearance and quasisingle helicity states of the reversed field pinch," *Phys. Rev. Lett.* **85**, 3169 (2000).
- ⁷S. Cappello and D. F. Escande, "Bifurcation in viscoresistive MHD: The Hartmann number and the reversed field pinch," *Phys. Rev. Lett.* **85**, 3838 (2000).
- ⁸S. Cappello, D. Bonfiglio, and D. F. Escande, "Magnetohydrodynamic dynamo in reversed field pinch plasmas: Electrostatic drift nature of the dynamo velocity field," *Phys. Plasmas* **13**, 056102 (2006).
- ⁹D. A. Ennis, D. Craig, S. Gangadhara, J. K. Anderson, D. J. Den Hartog, F. Ebrahimi, G. Fiksel, and S. C. Prager, "Local measurements of tearing mode flows and the magnetohydrodynamic dynamo in the Madison symmetric torus reversed-field pinch," *Phys. Plasmas* **17**, 082102 (2010).
- ¹⁰H. Biglari, P. H. Diamond, and P. W. Terry, "Influence of sheared poloidal rotation on edge turbulence," *Phys. Fluids B* **2**, 1 (1990).
- ¹¹T. S. Hahm and K. H. Burrell, "Flow shear induced fluctuation suppression in finite aspect ratio shaped tokamak plasma," *Phys. Plasmas* **2**, 1648 (1995).
- ¹²K. Burrell, "Effects of $E \times B$ velocity shear and magnetic shear on turbulence and transport in magnetic confinement devices," *Phys. Plasmas* **4**, 1499 (1997).
- ¹³P. W. Terry, "Suppression of turbulence and transport by sheared flow," *Rev. Mod. Phys.* **72**, 109 (2000).
- ¹⁴M. J. Lee, J. Kim, and P. Moin, "Structure of turbulence at high shear rate," *J. Fluid Mech.* **216**, 561 (1990).
- ¹⁵P. W. Terry, D. E. Newman, and N. Mattor, "Coherence of intense localized vorticity in decaying two-dimensional Navier-Stokes turbulence," *Phys. Fluids A* **4**, 927 (1992).
- ¹⁶J. C. R. Hunt and P. A. Durbin, "Perturbed vortical layers and shear sheltering," *Fluid Dyn. Res.* **24**, 375 (1999).
- ¹⁷M. Gobbin, D. Bonfiglio, D. F. Escande, A. Fassina, L. Marrelli, A. Alfieri, E. Martinez, B. Momo, and D. Terranova, "Vanishing magnetic shear and electron transport barriers in the RFX-mod reversed field pinch," *Phys. Rev. Lett.* **106**, 025001 (2011).
- ¹⁸P. W. Terry and K. W. Smith, "Coherence and intermittency of electron density in small-scale interstellar turbulence," *Astrophys. J.* **665**, 402 (2007).
- ¹⁹J. W. Connor, T. Fukuda, X. Garbet, C. Gormezano, V. Mukhovatov, M. Wakatani, ITB Database Group, and ITPA Topical Group, "A review of internal transport barrier physics for steady-state operation of tokamaks," *Nucl. Fusion* **44**, R1 (2004).
- ²⁰P. W. Terry, D. E. Newman, and A. S. Ware, "Local particle flux reversal under strongly sheared flow," *Phys. Plasmas* **10**, 1066 (2003).
- ²¹E.-J. Kim, "Role of magnetic shear in flow shear suppression," *Phys. Plasmas* **14**, 084504 (2007).
- ²²T. S. Hahm, "Physics behind transport barrier theory and simulations," *Plasma Phys. Controlled Fusion* **44**, A87 (2002).
- ²³R. D. Hazeltine and J. D. Meiss, *Plasma Confinement* (Dover Publications, Inc., 2003).
- ²⁴J. C. Bowman, J. A. Krommes, and M. Ottaviani, "The realizable Markovian closure. I. General theory, with application to three-wave dynamics," *Phys. Fluids B* **5**, 3558 (1993).
- ²⁵C. M. Bender and S. A. Orszag, *Advanced Mathematical Methods for Scientists and Engineers* (McGraw-Hill, 1978).
- ²⁶J. Wesson, *Tokamaks*, 3rd ed. (Oxford University Press, 2004).
- ²⁷G. Bateman, *MHD Instabilities* (The MIT, 1978).
- ²⁸S. Ortolani and D. Schnack, *Magnetohydrodynamics of plasma relaxation* (World Scientific, Singapore, 1993).
- ²⁹P. Martin, L. Apolloni, M. Puiatti *et al.*, "Overview of RFX-mod results," *Nucl. Fusion* **49**, 104019 (2009).